Process Safety and Environmental Protection 197 (2025) 107018

Contents lists available at ScienceDirect

Process Safety and Environmental Protection

journal homepage: www.journals.elsevier.com/process-safety-and-environmental-protection

Multiparametric resilience assessment of chemical process systems incorporating process dynamics and independent protection layers

Hao Sun [a], Meng Qi [b,*], Ming Yang [c,*], Fuyu Wang [a], Heping Wang [a]

[a] School of Management Science and Engineering, Anhui University of Technology, Ma'anshan, Anhui 243002, China
[b] College of Chemistry and Chemical Engineering, China University of Petroleum (East China), Qingdao 266580, China
[c] Safety and Security Science Section, Department of Values, Technology, and Innovation, Faculty of Technology, Policy, and Management, Delft University of Technology, the Netherlands

ARTICLE INFO

Keywords:
Resilience
Process safety
Independent protection layers
Hazardous operation

ABSTRACT

Chemical Process Systems (CPSs) exhibit complex characteristics and inherent dangers that can lead to serious accidents when disrupted. Accurate quantification and assessment of system resilience are crucial for effectively responding to potential undesired events. To address this, we propose a multiparametric resilience assessment methodology for CPSs that considers system dynamics and Independent Protection Layers (IPLs). This method integrates multiple CPS parameters using the Best Worst Method (BWM) to establish a comprehensive performance indicator. A dynamic simulation model incorporating IPLs is developed to monitor real-time changes in system parameters under disruptive influences. Additionally, a resilience metric is introduced, utilizing time-varying parameters to quantify system resilience under various disruptions. A case study involving a two-column pressure-swing distillation process with top recycling, designed to separate a minimum-boiling azeotrope of tetrahydrofuran and water, demonstrates the applicability of this method to complex CPSs. The results indicate that, compared to traditional resilience assessment methods based on reliability, the proposed approach provides time-dependent process parameters, reducing the uncertainty of reliability data. Furthermore, by considering IPLs, this method offers valuable decision support for the design and optimization of these protective layers.

1. Introduction

Chemical process systems (CPSs) encompass various stages, including production, processing, and storage, all of which involve numerous hazardous substances. These substances carry inherent risks, such as the potential for fire, explosion, and poisoning. Consequently, prioritizing the safety of CPSs is essential for their daily operation and management (Khan et al., 2021; Pasman et al., 2023; Sun et al., 2024).

A series of risk assessment methodologies and management strategies have been put forward to ensure system safety of CPSs (Zio, 2018; Aven and Zio, 2021; Reniers et al., 2018; Li et al., 2023). Khan and Amyotte (2007) built detailed modeling results based on quantitative risk assessment (QRA) and utilized three approaches and explosion modeling tools to investigate BP Texas City refinery incident. Zarei et al. (2023) combined Interval-Valued Spherical Fuzzy Sets (IVSFS) and Best Worst Method to propose a systematic approach to determine performance shaping factors and quantify their importance level and influence on the performance of the function of CPSs. Wen and Khan (2024) developed a risk-based model to evaluate and reduce conflict risks of a two-phase separator system. Cui et al. (2023) presented a rigorous dynamic process model to investigate various layers of protection, including basic process controls, alarms, safety instrumented systems, and pressure relief systems. The study evaluates their impact on accident prevention and assesses the dynamic safety performance and effectiveness of these protection layers. Zarei et al. (2024) discussed the key role of expert judgment in revealing the inherent complexity of socio-technical systems and addressing the challenges posed by uncertainty. Additionally, how approaches contribute to probability assessment and the representation of uncertainty has been illustrated. Qian et al. (2024) introduced the Inherent Process Risk Index (IPRI) methodology to assess the inherent safety of industrial processes. The review of the literature indicates that risk assessment is valuable for evaluating the probability and consequences of potential incidents. It supports the design of process system safety measures and emergency preparedness decisions,

* Corresponding authors.
E-mail addresses: qimeng@upc.edu.cn (M. Qi), m.yang-1@tudelft.nl (M. Yang).

https://doi.org/10.1016/j.psep.2025.107018
Received 1 December 2024; Received in revised form 31 January 2025; Accepted 9 March 2025
Available online 10 March 2025

ultimately enhancing overall system safety. Kamil et al. (2023) proposed a knowledge-based methodology to analyze fire and explosion accident likelihood. The natural language processing and interpretive structure model is used to extract effective information from accident database. Then, the probability method is utilized to analyze accident. It can be seen that risk assessment emphasizes the probability and consequences of accidents. It supports the establishment of safety barriers and management strategies to reduce risks.

However, to increase the scale and productivity of the system, CPSs become more complex and interdependent. But it also makes process systems vulnerable to uncertain disruptions (e.g., human errors, component failures etc.). Meanwhile, the accidents that have occurred indicate that disruptions are difficult to avoid completely. Consequently, under the influence of disruptive events, how to ensure that the system functionality remains at a high level has become an urgent challenge that needs attention (Sun et al., 2022; Yang et al., 2023; Li et al., 2024). Evaluating how a system absorbs and adapts to disruptions while quickly recovering from them is key to addressing this challenge. Therefore, more attentions should be paid on resilience assessment because it encompasses a broader perspective, considering the ability of CPSs to maintain functionality and quickly recover from disruptions. Furthermore, the persistence of accidents within CPSs suggests that disruptive events are an inevitable reality (Misuri and Cozzani, 2021; Liu et al., 2024; Meng et al., 2024), highlighting a critical need for a revised approach. The underlying causes for this include:

(1) CPSs function under stringent conditions, requiring precise control of parameters like temperature, pressure, flow rate, and liquid level within safety limits. Deviations can disrupt processes, potentially causing accidents and halting production (Pawar et al., 2022).
(2) Modern CPSs feature a complex, highly integrated design, leading to dependencies among components. This interconnectedness boosts efficiency but also increases vulnerability to disruptions, where a failure in one part can trigger cascading failures across the system (Bellè et al., 2023).
(3) CPSs face diverse and unpredictable disruptive events, including natural disasters, mechanical failures, cyber-attacks, and sabotage, marked by their uncertain and dynamic nature. Predicting the specifics of these disruptions is challenging, with the potential for widespread and evolving impacts (Xu et al., 2024; Jain et al., 2018; Hu et al., 2021).

Consequently, ensuring resilience against all types of disruptions is a priority for CPSs. The assessment and improvement of CPS resilience are crucial for maintaining production sustainability and safeguarding system safety (Amer et al., 2023). Although resilience lacks a universally agreed-upon definition (Szatmári et al., 2024), it has garnered significant interest across various sectors, including transportation (Tang et al., 2022), power grids (Ouyang et al., 2019), nuclear power (Yan et al., 2023), mechanical systems (Cai et al., 2021), and process systems (Cincotta et al., 2019).

In the domain of CPSs, resilience refers to the capability of the system to absorb, adapt to, and recover from the adverse impacts of disruptive events (Chen et al., 2023). The concept of resilience emphasizes the proactive enhancement of the ability of a system to handle disruptions, thereby fostering safety under complex conditions (Sharma et al., 2018). To achieve this, various approaches for assessing resilience have been developed. Jain et al. (2018) presented resilience-based integrated process systems hazard analysis (RIPSHA) framework, including four resilience aspects, namely early detection, error tolerant design, plasticity, and recoverability. Yazdi et al. (2022) proposed a probabilistic resilience assessment methodology for subsea pipeline based on Markov chain and dynamic Bayesian network (DBN). Yang et al. (2023) developed a resilience assessment framework for CPSs that considers disruption, functionality, performance, and uncertainty. Zeng et al. (2022) discussed the complex mechanism of Natech domino effects and explored the propagation pattern. Based on this, some resilience enhancement strategies, such as safety barriers management, are proposed. Pawar et al. (2022) introduced a resilience framework based on reliability for resilience assessment of fast response process systems. To enhance resilience, design modifications and operational interventions are investigated. Sun et al. (2022) presented a dynamic Bayesian network (DBN)-based methodology for assessing and improving the resilience of CPSs, with system availability serving as the performance metric. Zhang et al. (2025) raised a resilience-driven optimization methodology for the emergency maintenance operation scheme of subsea production system, considering maintenance operational risk. Tong and Gernay (2023) developed a resilience assessment framework of facilities vulnerable to cascading accidents in the process industry. The BN is utilized to assess the impacts of protection measures on the resilience to fire hazard. Yazdi et al. (2024) introduced a holistic taxonomy of resilience performance and raised a qualitative resilience assessment framework using a novel Intuitionistic fuzzy Weighted Influence Nonlinear Gauge System (IFWINGS) to address the uncertainty and variability of expert opinion in resilience assessments. Hoseyni and Cordiner (2024) presented a DBN-based methodology to assess the resilience of green hydrogen plant. DBN is used to quantify the systen resilience at the early and late design stages. Lastly, Cincotta et al. (2019) developed a resilience assessment methodology for firefighting strategies in CPSs, through which the optimal strategy was determined through failure probabilities of tanks derived from Bayesian networks and probit functions.

The literature review reveals notable limitations in current methods on CPSs resilience assessment: (1) While probability, reliability, and availability are commonly used as resilience performance indicators for CPSs, methods based on these metrics typically rely on past experience and encounter data uncertainty; (2) Current assessment methods overlook the role of system protections, which are essential for preventing accidents and mitigating the negative impacts of disruptive events on CPSs (Cui et al., 2023). Incorporating the function of independent protection layers (IPLs), which absorb and adapt to disruptions to prevent accidents, is crucial for a comprehensive evaluation of a system true resilience. In addition, CPS accidents are frequently precipitated by deviations in process parameters, such as temperatures, pressures, and flow rates, deviating from their safety thresholds (Hoseyni and Cordiner, 2024). Directly monitoring these system parameters offers a more immediate and accurate reflection of how a system performance varies in response to disruptions. Moreover, since system parameters can be derived from time-dependent process data, leveraging them can significantly reduce the impact of data uncertainty. Yet, few studies have evaluated resilience using multiple process parameters, and none have explored deviation propagation in complex CPSs, a factor that introduces significant challenges to multiparametric resilience assessment.

Given the discussions, there is a critical need for evaluating the resilience of CPSs that incorporates system dynamics, which offer insights into how CPSs react to various disruptions, showcasing the effectiveness of built-in protections and the significance of time-varying system parameters in reflecting dynamic resilience performance. To this end, dynamic process simulation emerges as a vital tool for capturing system dynamics across different disruptive scenarios, especially given the increasing complexity and integration of CPSs (Lee et al., 2024). The escalating complexity of CPSs, alongside the development of model-based safety approaches and advancements in simulation technology, has spurred the application of dynamic process simulation to enhance process safety assessments across various domains (Luyben, 2012). As a result, dynamic process simulation has been adopted by the Process Safety Engineering Community to enhance safety analyses of CPSs, including HAZOP (Janošovský et al., 2017), layers of protection analysis (LOPA) (Cui et al., 2023), and QRA (Ko, et al., 2020). The primary benefit of dynamic process simulation is its ability to simulate

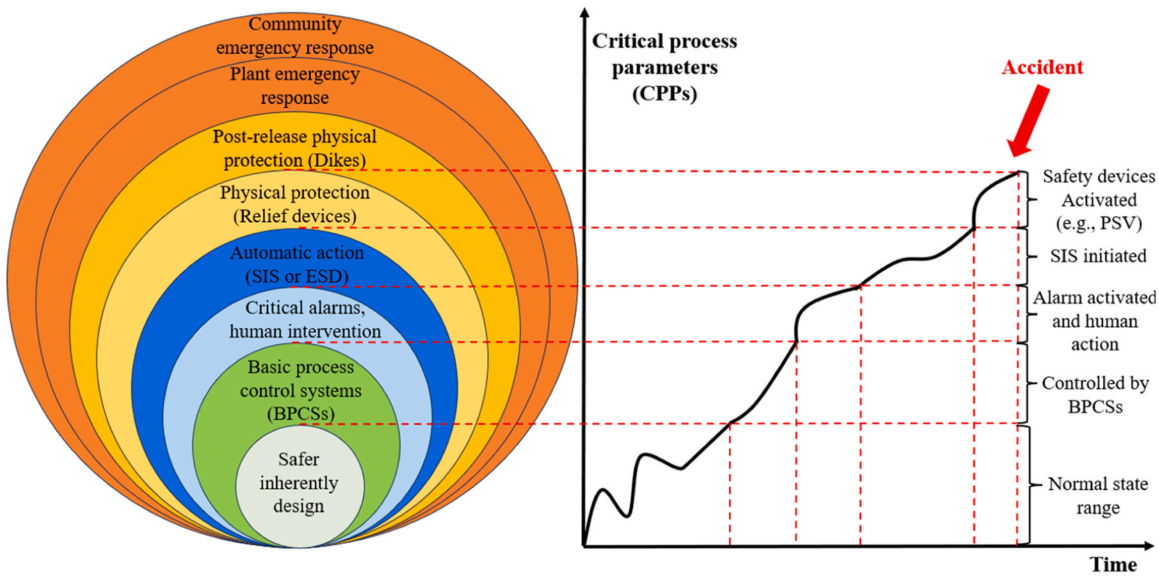

Fig. 1. The relationship between independent protection layers and system process parameters.

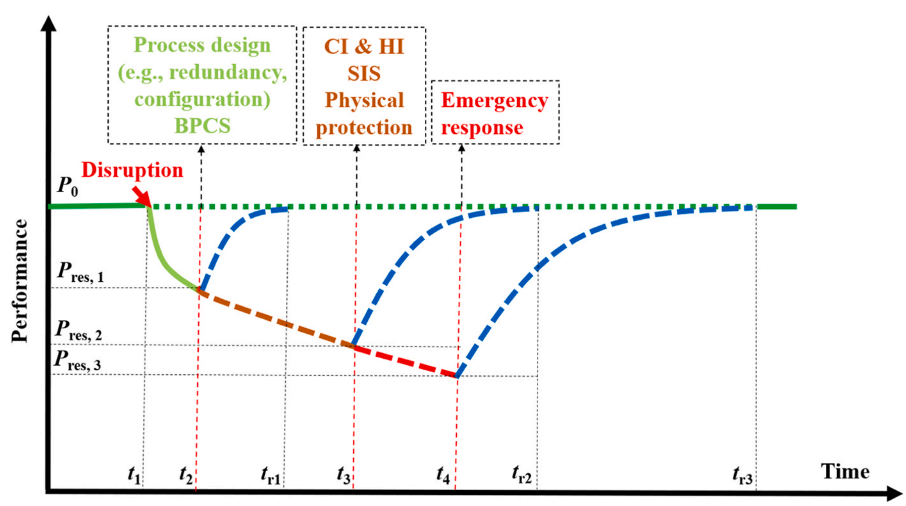

Fig. 2. The role of protection layers in system performance.

real system dynamics, incorporating control actions and protections, which is crucial for assessing system resilience right from the conceptual design phase. Thus, leveraging dynamic process simulation to simulate system dynamics under various protections is essential for a thorough resilience assessment of CPSs.

In this study, we introduce an approach based on dynamic process simulation for a comprehensive assessment of CPS resilience based on multiple process parameters, integrating system dynamics and Independent Protection Layers (IPLs). This method employs dynamic process simulation, incorporating IPLs to capture the real dynamics of the system under specific disruptive scenarios, facilitating the collection of time-varying multiparametric process data. We then devise a novel strategy to synthesize this multiparametric data into a performance response function (PRF) that reflects the system's resilience behavior. Finally, the system's resilience is assessed by examining various disruption scenarios in conjunction with IPLs. The key contributions of this work are summarized as follows:

1. We propose an approach for assessing resilience that leverages dynamic simulation, integrating system dynamics with IPLs. To the author's knowledge, this is the first study includes add-on protections systematically in CPS resilience assessment.
2. A strategy for synthesizing multiple parameters is developed, utilizing the best-worst method. This introduces a multiparametric-based performance indicator designed to address the challenges posed by deviation propagation and variations in system parameters.
3. We conduct an extensive resilience assessment of an integrated distillation system, taking into account a variety of protections including basic controls, alarms, and safety instrumented systems.

2. Preliminary

2.1. Independent protection layers (IPLs)

In the event of a disruption, a system performance will begin to decline without protective measures or interventions, potentially impairing its functionality over time. Therefore, protective measures play a crucial role in ensuring the continuity of operations and averting accidents within CPSs. IPLs are critical components in this context, consisting of devices, systems, or actions specifically designed to prevent a potentially hazardous scenario from resulting in undesirable

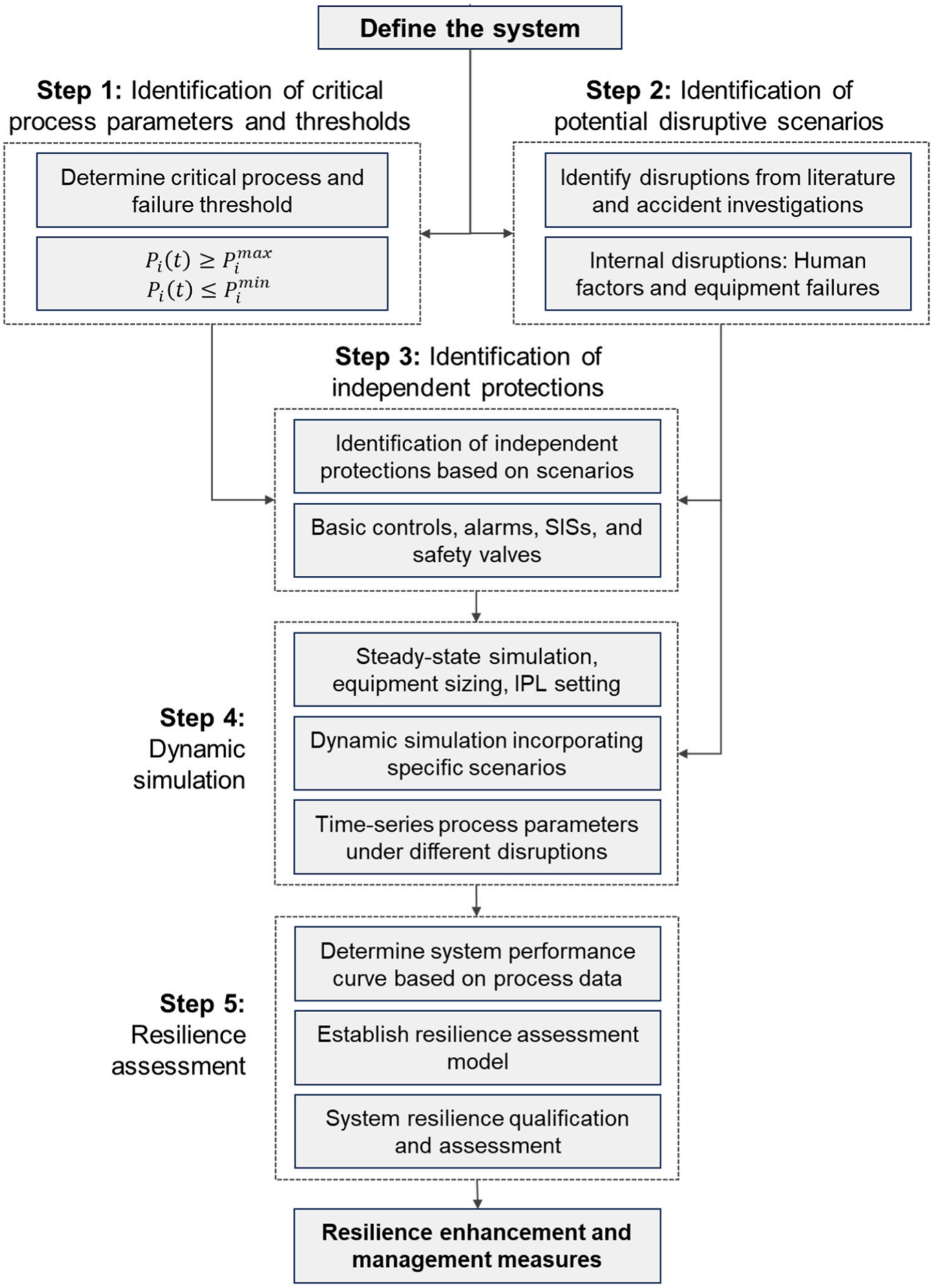

Fig. 3. Proposed approach for multiparametric resilience assessment.

outcomes. The independence means their operational effectiveness is not influenced by the initial cause of the scenario or by the failure of other protection layers (Dowell, 2019; Li, et al., 2022). The general principle is to ensure functional independence, physical independence, operational independence, and independence in maintenance.

To mitigate hazards, inherently safer design principles are applied to the process design, aiming to eliminate or significantly reduce risks within the process system. Nonetheless, process design alone cannot guarantee complete system safety. In response to deviations triggered by disruptions, the basic process control system (BPCS) is employed to adjust system parameters back to their normal ranges. Should the BPCS fail, process parameters may reach critical levels, triggering a critical alarm (CA). This, in turn, necessitates human intervention (HI) to either return the process to a safe state or initiate a plant shutdown. However, due to the potential for CA reliability issues and human errors, CA and HI cannot be solely relied upon for safety. As a result, a safety instrumented system (SIS) is implemented as an additional safeguard. Designed to operate independently from the BPCS, the SIS activates interlocks to halt feed and/or steam inputs when process parameters exceed SIS thresholds. In the event that the SIS is unable to respond during an emergency, physical protections such as pressure safety valves (PSVs) serve as the ultimate defense against accidents. Fig. 1 illustrates how IPLs interact with the time-dependent process parameters of the system.

System performance is gauged using multiple time-varying parameter data. Disruptions lead to variations in performance over time, as illustrated in Fig. 2. Initially, the system operates within a safe performance range. Upon encountering disruptions, process design elements like redundancy and configuration, alongside the BPCS, work to mitigate the disruption impact. Ideally, a system should be resilient enough to counteract all disruption effects. Yet, designing a system fully impervious to such impacts is challenging. Thus, when a disruption intensity overwhelms the mitigation capacity of the process design and BPCS, there is a noticeable decline in system performance. At this juncture, CA & HI and the SIS play crucial roles in adapting and restoring system performance, aiming to lessen the disruption's impact. The importance of IPLs in maintaining safe system performance is evident. Assessing system resilience with a focus on IPLs is essential for ensuring ongoing safety and production continuity.

2.2. Process simulation

In the past, chemical process designs were simple enough that qualitative and knowledge-based safety assessments were both efficient and cost-effective. However, as these processes have evolved to improve material and energy efficiencies—by incorporating material recycles, integrated heat and power systems, frequent adjustments to operating points, and advanced control systems—their complexity has greatly increased. This added complexity means that traditional safety methods, which depend on a thorough understanding of process hazards, may no longer be adequate for today's more intricate processing environments. Modern process safety now involves complex interactions and dependencies within the system, making traditional safety assessments less straightforward and more subjective. (Zhu et al., 2020; Leveson and Stephanopoulos, 2014).

Process simulations can model intricate processes, including reactions, separations, heat and mass transfer, and control systems. This would support safety assessment by providing better understanding of how these systems behave under normal and abnormal situations. Process simulation offers detailed insights into hazard interactions and their dynamic characteristics within the process, viewed from a systemic perspective (Janošovský et al., 2019). Process simulations allow for the exploration of numerous "what-if" scenarios to illustrate how deviations originating in one system component can spread through system units and evaluate the effectiveness of IPLs in controlling these deviations (Kummer and Varga, 2019).

In the current study, process simulations enable resilience assessment of CPSs at the conceptual design stage and provides how system resilience can be improved by adopting different configurations and actions. Simulations can help to validate the performance of safety measures under various conditions, ensuring they function as intended during actual incidents. The robustness of the simulation model can vary based on the level of detailed information available, allowing it to meet the assessment requirements at different stages of the design process. The market offers a variety of simulation tools, including CHEMCAD, Aspen Tech (Aspen Plus, Aspen HYSYS, Aspen Dynamics), PRO/II, gPROMS, and Matlab/Simulink, providing diverse options for conducting detailed performance analyses under various disruptive scenarios.

3. The proposed approach

This section details the proposed multiparametric resilience assessment approach for CPSs based on performance response curve, which is presented in Fig. 3. It mainly includes five parts: (1) Identification of critical process parameters and thresholds; (2) identification of potential disruptive scenarios; (3) identification of independent protections; (4) dynamic simulation; and (5) resilience assessment.

3.1. Identification of critical process parameters and thresholds

The determination of critical process parameters (CPPs) is vital for quantifying process resilience, as these parameters represent a set of operating variables that reflect the operational safety of the CPS. CPPs have thresholds; if these are exceeded, the system's operation becomes unsafe. In CPSs, most accidents originate from deviations in process parameters such as pressure, temperature, flow rate, and level. Typically, pressure and temperature are crucial for determining safe operating conditions, thus serving as CPPs. An abnormal event occurs when process parameters reach their normal operating limits at any point in time. Hence, for a CPP P_i, a potential disruptive event F can be defined as:

$$P_i(t) \geq P_i^{\max} or P_i(t) \leq P_i^{\min}, \forall t \in T \tag{1}$$

where P_i^{up} and P_i^{low} represent the upper and lower operating limits for the CPPs. These limits are typically defined according to controllable ranges of the BPCS.

3.2. Identification of potential disruptive scenarios

Disruptions can be categorized as external disruptions (e.g., natural disasters and cyber-attacks) and internal disruptions (e.g., human factors and equipment failures). According to literature and accidents investigations, the frequency of external disruptions in the chemical process systems is quite low. On the other hand, about 75 % of incidents in process industries occurred during operations and most of these incidents are caused by human factors and equipment failures (Wang et al., 2021). Thus, more attention should be concentrated on human factors and equipment failures.

Human factors and equipment failures can occur to any system component with an even unknown probability (Zio, 2022). For human factors, the impact of this type of disruptions on the system is reflected in the variation of the system process parameters caused by human causes. Equipment failures refer to the failure of equipment, instruments, valves, etc., to perform their intended functions successfully. This kind of disruption will directly affect the system operation. In particular, critical safety devices, once failed, may lead to fire or explosion accidents.

The potential disruptive events should be determined based on historical accident reports and related literature in the chemical process industry. Eventually, those disruptions can be characterized by deviations in process parameters. Once the deviation exceeds the threshold, as shown in Eq. (1), it may lead to an accident.

3.3. Identification of independent protections

According to the identified disruptive scenarios, the independent protections correspond to specific disruptive scenarios and parameter deviations. This process involves a thorough analysis of the system process flowsheet and designs to pinpoint specific protections that can effectively respond to potential disruptive scenarios and deviations in critical process parameters. The protections encompass a range of mechanisms, including basic process controls that maintain the operational stability of the system, alarms and human intervention strategies that provide timely alerts and corrective actions, advanced SISs that automatically engage to mitigate risks, and safety valves designed to prevent overpressure conditions. These should be identified to comprehensively reflect the system ability to encounter potential disruptions. Each of identified protections should work independently to prevent critical parameters from reaching unacceptable levels. All the independent protections will be incorporated into process simulation to demonstrate their response and function in preventing hazardous scenarios.

3.4. Dynamic simulations

Dynamic simulations play a pivotal role in understanding the behavior of process systems under various disruption scenarios. In this study, we have chosen the commercial software Aspen Dynamics for our process simulations, building upon our previous work's methodology that emphasizes modeling CPSs with IPLs. The approach begins with the development of a steady-state simulation model in Aspen Plus, which is essential for establishing mass and heat balances and thus, crucial for accurately sizing the necessary equipment. This steady-state model serves as a foundation and is subsequently transformed into a dynamic model within Aspen Dynamics. This transformation involves the integration of various control mechanisms and independent protections, including emergency hand valves, SISs, and pressure relief valves. The primary objective of this dynamic simulation is to accurately reflect the process behavior under disruptions and hazardous conditions, taking into consideration the dynamic responses of the system and the proactive measures provided by the IPLs. This comprehensive approach ensures a more robust and reliable understanding of the process dynamics, enhancing accurate assessment of system resilience.

3.5. Resilience assessment

3.5.1. Quantification of system performance curve

(1) Normalization of time-dependent data of CPPs

CPPs can be categorized into two types, namely safety CPPs (e.g., pressure and temperature) and production related CPPs, like production purity, productivity, energy consumption, and etc. All types of CPPs will change with time when the system is impacted by disruptive events. Only one of them cannot comprehensively reflect the system performance variation. Therefore, the system performance curve should be represented by an integrated performance indicator that considers with all CPPs.

Due to the difference in numerical dimensions between diverse CPPs, it, therefore, is indispensable to normalize the time-dependent CPPs. Then, the CPPs of the system can be described as dimensionless variable between 0 and 1. According to the expected value, actual value and upper and lower limit values of the CPPs, the time-dependent system data is processed by Eq. (2) when P_{rt} is greater than P^*. Otherwise, the time-dependent process data is processed by Eq. (3) when P_{rt} is less than P^*. The range of normalized data is [0,1]. 0 indicates that the system is in the failure state, and 1 represents that the system is in the highest performance state.

$$\phi(t) = 1 - \frac{P_{rt} - P^*}{P_{Max} - P^*} \tag{2}$$

$$\phi(t) = 1 - \frac{P^* - P_{rt}}{P^* - P_{Min}} \tag{3}$$

where ϕ refers to system performance after normalization, P_{rt} is the measured value of the system parameters; P^* is the expected value for normal operating conditions; P_{Max} is the maximum acceptable upper limit; P_{Min} is the minimum acceptable lower limit. It should be noted that because the BPCS could offset minor deviations in system parameters, therefore P^* is modified as a reasonable range corresponding to the upper and lower operating limits of the BPCS, which are mentioned previously as P_i^{up} and P_i^{low}, respectively. If the system parameters fall into this range, ϕ is considered as 1.

Suppose the system has m CPPs (P_1, P_2, …, P_m), the normalized data of CPPs is defined as ϕ_1, ϕ_2, …, ϕ_m. To comprehensively reflect the system performance under disruptive events, the system performance indicator can be depicted as Eq. (4).

$$\phi(t) = k_1\phi_1(t) + k_2\phi_2(t) + \cdots + k_m\phi_m(t) \tag{4}$$

where k_1 refers to the weight of P_1, $k_1 + k_2 + \ldots + k_m = 1$, ϕ stands for the aggregated system performance indicator.

(2) Best worst method (BWM)

Although the comprehensive performance indicator is influenced by all CPPs, their contributions may not be evenly distributed. Consequently, it is essential to assign weights to each CPP to reflect their respective contributions to the overall performance indicator.

The BWM is an efficient way to assign weights to different CPPs (Rezaei, 2015). Compared to other multi-criterion decision-making (MCDM) methods, BWM not only requires less pairwise comparison between factors, reduces the time required for analysis, and can also produce more reliable results (Wu et al., 2024). For n factors, compared with the pairwise comparison number $n(n\text{-}1)/2$ of other MCDM methods, the number of pairwise comparisons of BWM is $2n\text{-}3$. As a result, it has the advantage that consistent results can be obtained with less comparative information. In this work, BWM is utilized to acquire weights of each CPP. The main steps of BWM are shown as follows:

Step 1: Determine decision criteria. A series of decision criteria should be defined and employed to make a decision. In this study, the decision criteria are CPPs (e.g., {pressure P_1, temperature P_2, production purity P_3, productivity P_4, energy consumption P_5, and etc.} of the system.

Step 2: Identify the best and the worst criteria. Take a reactor as an example, its internal pressure directly determines the safety of the reactor, so the temperature (P_2) can be regarded as the best criteria. The energy consumption (P_5) can be viewed as the worst one.

Step 3: Determine the priority of the best criterion compared to all other criteria, ranging from 1 to 9. The corresponding Best-to-others vector can be depicted as: $A_B = (a_{B1}, a_{B2}, \cdots, a_{Bn}),$.

where a_{Bj} represents the priority of the best criterion over the criteria j.

Step 4: Determine the priority of all other criteria compared to the worst criterion, ranging from 1 to 9. The corresponding Others-to-worst vector can be represented as: $A_W = (a_{1W}, a_{2W}, \cdots, a_{nW})^T$,

where a_{Bj} represents the priority of the best criterion over the criteria j.

Step 5: Determine the optimal weights (w_1^*, w_2^*, …, w_n^*).

The optimal weight of the criteria is that for each pair of w_B/w_j and w_j/w_W, $w_B/w_j = a_{Bj}$ and $w_j/w_W = a_{jW}$ are satisfied. To satisfy these conditions for all j, a solution should be found to make the maximum absolute differences $\left|\frac{w_B}{w_j} - a_{Bj}\right|$ and $\left|\frac{w_j}{w_W} - a_{jW}\right|$ of all j is minimized. Thus, the problem can be represented as Eq. (5).

$$\begin{aligned} &\min \max_j \left\{ \left|\frac{w_B}{w_j} - a_{Bj}\right|, \left|\frac{w_j}{w_W} - a_{jW}\right| \right\} \\ &s.t. \\ &\sum_j w_j = 1, \\ &wj \geq 0, forallj \end{aligned} \tag{5}$$

Then, Eq. (5) can be changed into Eq. (6).

$$\begin{aligned} &\left|\frac{w_B}{w_j} - a_{Bj}\right| \leq \xi, forallj \\ &\left|\frac{w_j}{w_W} - a_{jW}\right| \leq \xi, forallj \\ &s.t. \\ &\sum_j w_j = 1, \\ &wj \geq 0, forallj \end{aligned} \tag{6}$$

By solving Eq. (6), the optimal weights (w_1^*, w_2^*, …, w_n^*) and ξ can be determined. After that, by combining Eq. (4) and Eq. (6), the comprehensive performance indicator can be depicted as Eq. (7). Then, the performance curve of the system can be obtained.

$$\phi(t) = {w_1}^*\phi_1(t) + {w_2}^*\phi_2(t) + \cdots + {w_m}^*\phi_m(t) \tag{7}$$

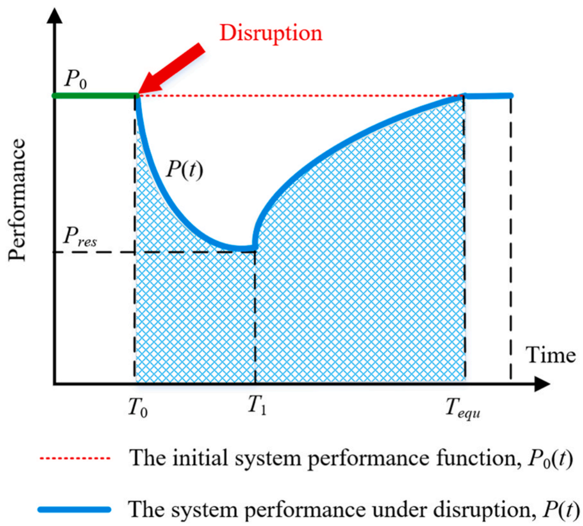

Fig. 4. The system performance curves under disruptive events.

3.5.2. *Resilience assessment based on system performance curve*

Once the system performance curve is obtained, as shown in Fig. 4, the system resilience can be measure and represented the ratio of the area under the performance curve $P(t)$ to the area under the initial performance curve from T_0 (disruption occurrence time) to T_{equ} (time to reach a new equilibrium state) (Pawar et al., 2022; Yang et al., 2023).

According to those studies, the system resilience can be depicted as Eq. (8).

$$\mathscr{R}(t|e^j) = \frac{\psi(t|e^l) - \psi(t_d|e^l)}{\psi(t_0) - \psi(t_d|e^l)} \tag{8}$$

where $\mathscr{R}(t|e^j)$ stands for system resilience at time t; $\psi(t|e^l)$ refers to the system performance at time t; $\psi(t_d|e^l)$ indicates the lowest performance of the system; $\psi(t_0)$ is the initial performance of the system. Eq. (8) can be converted into Eq. (9) by considering the time term. The overall resilience of the system can be represented as Eq. (10).

$$R(T_x) = \frac{\int_{T_0}^{T_x} P(t)dt}{\int_{T_0}^{T_x} P_0 dt} = \frac{\int_{T_0}^{T_x} P(t)dt}{P_0(T_x - T_0)} \tag{9}$$

$$R(T_{equ}) = \frac{\int_{T_0}^{T_{equ}} P(t)dt}{P_0(T_{equ} - T_0)} \tag{10}$$

where $R(T_x)$ is the system resilience at time T_x; T_x is the time between T_0 and T_{equ} ($T_0 < T_x < T_{equ}$); T_0 represents occurrence time of the disruption; P_0 represents the initial performance of the system; $P(t)$ stands for a new equilibrium performance of the system.

4. Case study

In CPSs, separation remains as an essential task for purifying products, and its process is generally complex with recycling streams if multi-component separation is required. For separation, distillation commonly serves as the key unit operation. To demonstrate the method applicable for complex CPSs, this study focuses on a case involving a two-column pressure-swing distillation (PSD) process with top recycling, designed to separate a minimum-boiling azeotrope of tetrahydrofuran (THF) and water. The presence of a recycle stream within the PSD process introduces the potential for exacerbated deviation propagation, as the recycle loop may generate secondary effects. Dynamic process simulation was conducted to capture the time-dependent behavior of CPPs

Table 1
Key operating parameters of the PSD system (Cui et al., 2020).

Parameter	Value
Feed temperature	30 °C
Feed flow rate	2000 kmol/h
Pressure of the LPC	0.533 bar
Pressure of the HPC	12.70 bar
Number of stages of the LPC	13
Number of stages of the HPC	23
LPC top/bottom temperature	46.0/86.9 °C
HPC top/bottom temperature	157.8/173.2 °C

Table 2
Summary of upper and lower limits of each CPP.

Parameter	Minimum limit	Normal range	Maximum limit
LPC pressure	-	0.5–0.55 bar	2.5 bar
HPC pressure	-	12.65–12.75 bar	17 bar
Water mole fraction	0.999	0.99999	-
THF mole fraction	0.99	0.9999	-

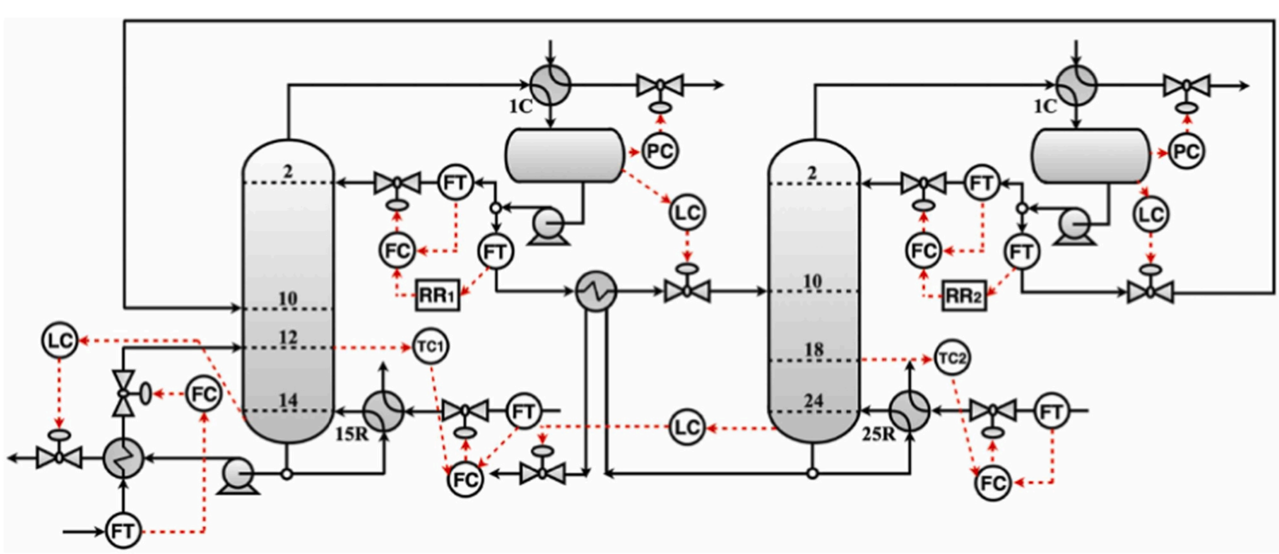

Fig. 5. Process configuration and associated control structure of the PSD.

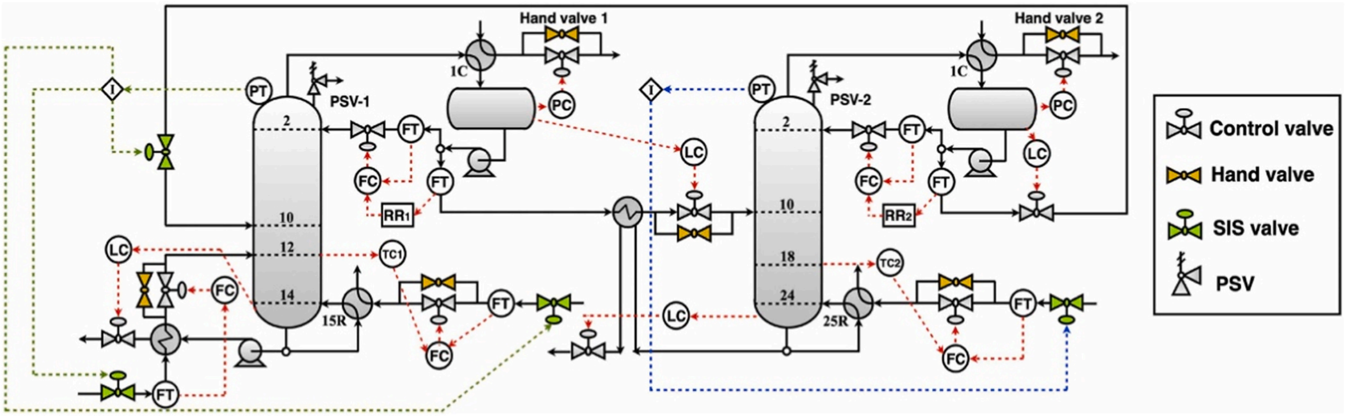

Fig. 6. Piping and instrumentation diagram (P&ID) of the PSD process.

Table 3
Activation setpoint of pressure for each IPL.

IPL	LPC activation pressure	HPC activation pressure
CA&HI	0.6 bar	13 bar
SIS	2.0 bar	15 bar
PSV	2.5 bar	17 bar

Table 4
Summary of investigated scenarios with IPL details.

Scenario	Disruption description	IPL description	Activated IPL
1	Loss of cooling water of the LPC	Operator opens the cooling water valve manually after receiving the alarm in 30 s/60 s/90 s	CA&HI
2	Loss of boiler water of the HPC	Operator opens the boiler water valve manually after receiving the alarm in 30 s/60 s/90 s	CA&HI
3	Loss of cooling water of the LPC	SIS activated when LPC pressure achieves 2 bar to shut down the feeds and steam	SIS
4	Loss of boiler water of the HPC	SIS activated when HPC pressure achieves 15 bar to shut down the steam	SIS

under various disruptive scenarios. This case study investigates the consequences of abnormal operations that could originate from human errors and equipment malfunctions. The considered consequences are overpressure and flooding, triggered by process deviations like coolant supply failures, sudden increases in heat input, and variations in feed flow rate and composition.

4.1. System description

The process flowsheet for the PSD process is illustrated in Fig. 5, featuring a low-pressure column (LPC) and a high-pressure column (HPC) designed for the separation of THF and water. This case was extracted from our previous publication, in which a rigorous dynamic safety analysis has been carried out for the PSD system (Cui et al., 2023). The system feed consists of 6/94 mol% THF/water, at a temperature of 30 °C and a flow rate of 2000 kmol/h. The target purities for THF and water are 99.99 mol% and 99.999 mol%, respectively. Under desired operating conditions, the LPC operates at 0.533 bar, while the HPC operates at 12.70 bar (Cui et al., 2020). A summary of the process operating parameters is shown in Table 1.

The PSD process utilizes steam-heated reboilers for heating and employs cooling water (as the case of LPC) as well as boiler condensate water (as the case of HPC) for condensation in two condensers, with the latter also recovering heat from the top of the HPC. The LPC bottom output is high-purity water, and the HPC bottom output is high-purity THF, with the HPC distillate being recycled to the LPC for material efficiency. In addition, the bottom streams of the LPC and HPC are heat exchanged with their column feed streams to enhance energy efficiency of the process.

To maintain reliable and stable operation of the process, various control loops are implemented acting as the BPCS: the total feed flow rate is regulated for throughput adjustment; the condenser pressures of both LPC and HPC are managed by adjusting coolant flow rates; the level in the reflux drum is controlled by altering the distillate flow rate; the flow rate of the column base is modified to manage the bottom level; the reflux ratio is maintained at a set value; and the temperatures at the LPC 12th stage and the HPC 18th stage are regulated by adjusting the flow rates of the heating or cooling medium.

4.2. Potential disruptions and critical system parameters

In distillation operations, overpressure and flooding represent significant safety risks which should be carefully managed. Column overpressure can result from a range of process deviations and failures, including utility disruptions like coolant loss, malfunctions in control systems, or manual operation errors such as pressure controller breakdowns. Other causes include heat exchanger failures, the buildup of non-condensable gases, or even internal explosions (Kister, 1997). Similarly, flooding occurs when there is excessive liquid retention within the column, leading to high vapor/liquid loadings. This condition is typically linked to fluctuations in tank levels, increased pressure drops across the column, and a reduction in mass transfer efficiency, all of which can significantly impact process safety and operational performance.

In light of the identified safety issues of overpressure and flooding, four potential disruptive scenarios were examined, primarily based on combining the factors mentioned above:

Disruption 1 (D1). : Loss of cooling medium in the LPC or HPC condenser.

Disruption 2 (D2). : Increased heating medium in the LPC or HPC reboiler.

Disruption 3 (D3). : Variations in the feed flow rate.

Disruption 4 (D4). : Variations in the THF content of the feed.

Disruptions D1 and D2 are linked to the consequence of potential overpressure in the columns, whereas D3 and D4 are associated with column flooding. To accurately assess the impact of these disruptions on system resilience performance, four CPPs have been identified: LPC pressure, HPC pressure, water mole fraction, and THF mole fraction. Monitoring the first two parameters is essential to prevent overpressure,

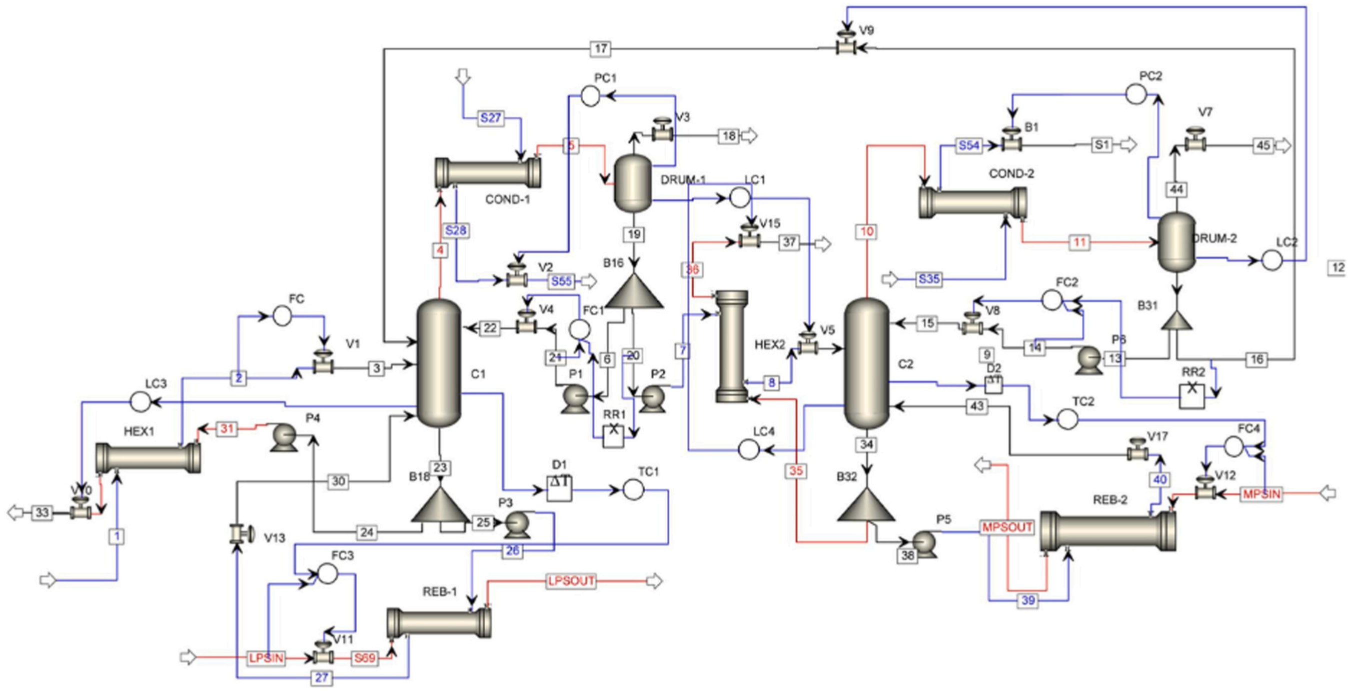

Fig. 7. Dynamic simulation model developed in Aspen Dynamics.

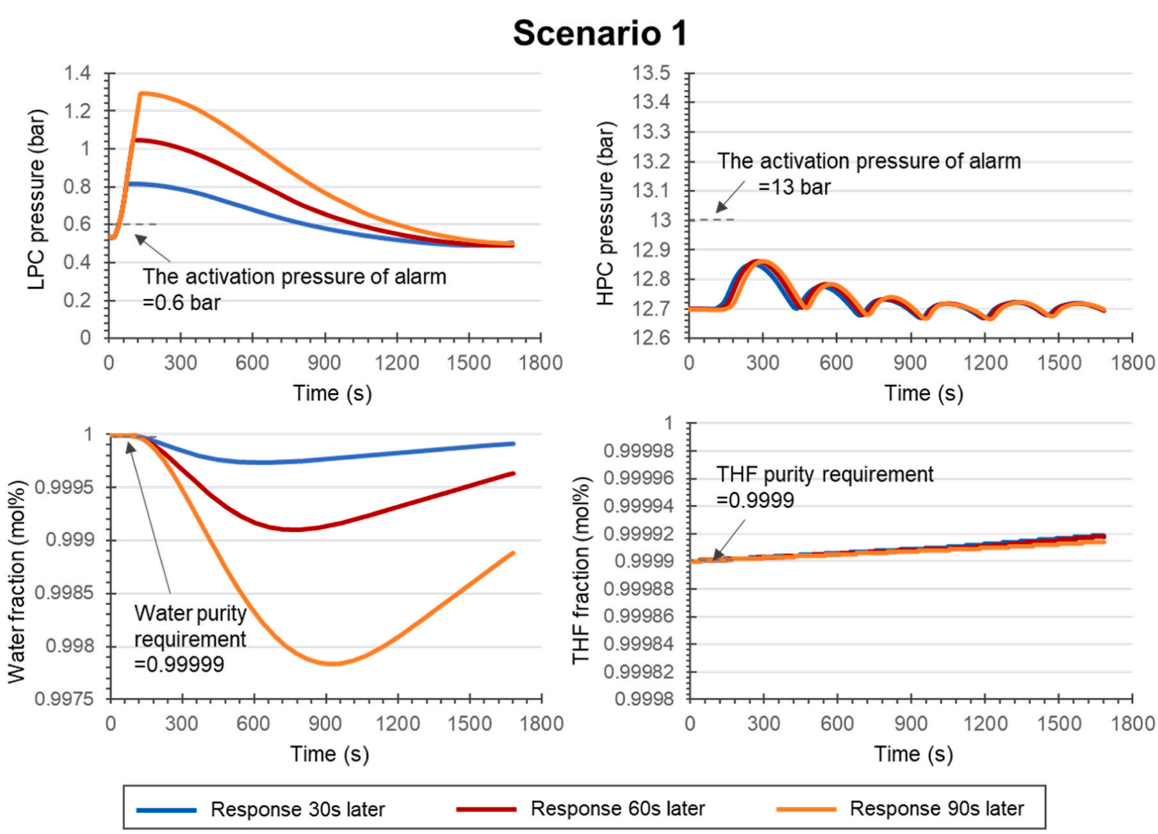

Fig. 8. Simulation results of Scenario 1.

while monitoring the latter two is crucial for preventing column flooding in the PSD process.

The thresholds for the aforementioned CPPs need to be determined. For LPC pressure and HPC pressure, these parameters have maximum limits, which are set at their activation pressure for pressure relief: 2.5 bar for LPC pressure and 17 bar for HPC pressure. The water mole fraction and THF mole fraction have minimum limits below which the product purity is not qualified. The minimum limits for the water mole fraction and THF mole fraction are 0.9999 and 0.999, respectively. These minimum limits are also determined at their activation pressure

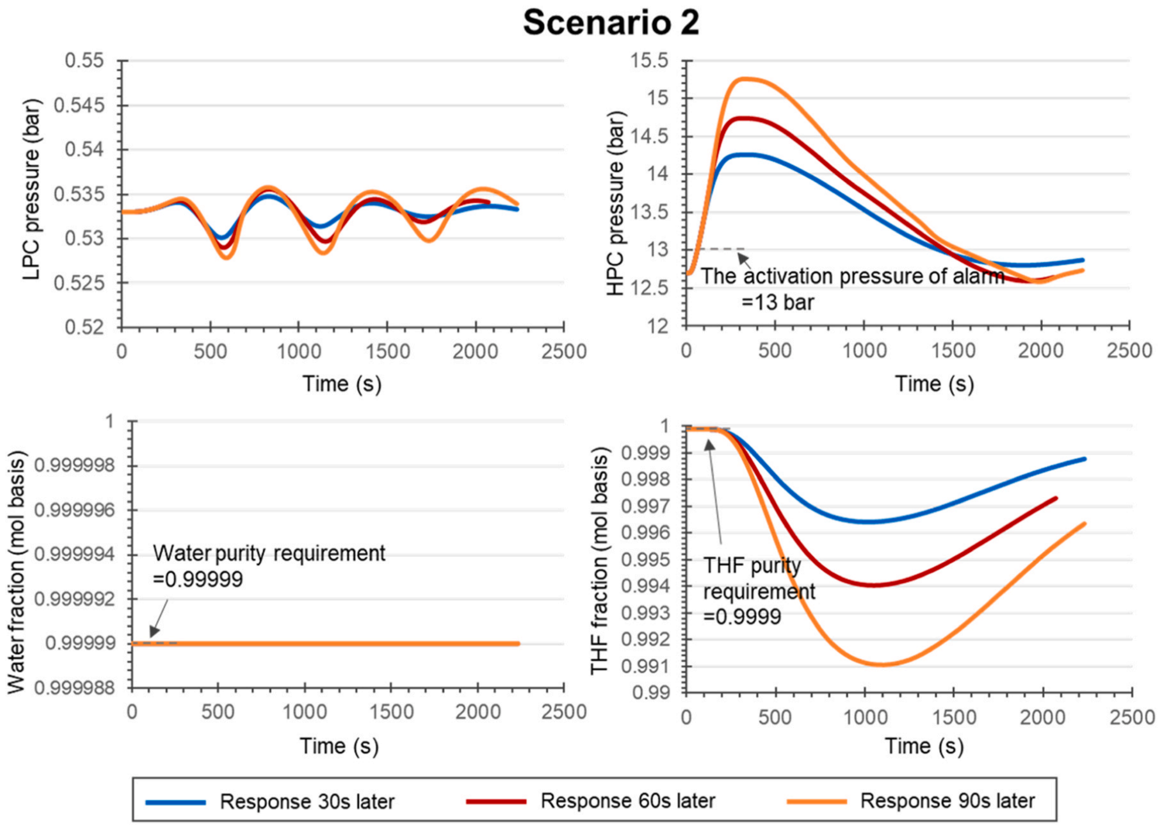

Fig. 9. Simulation results of Scenario 2.

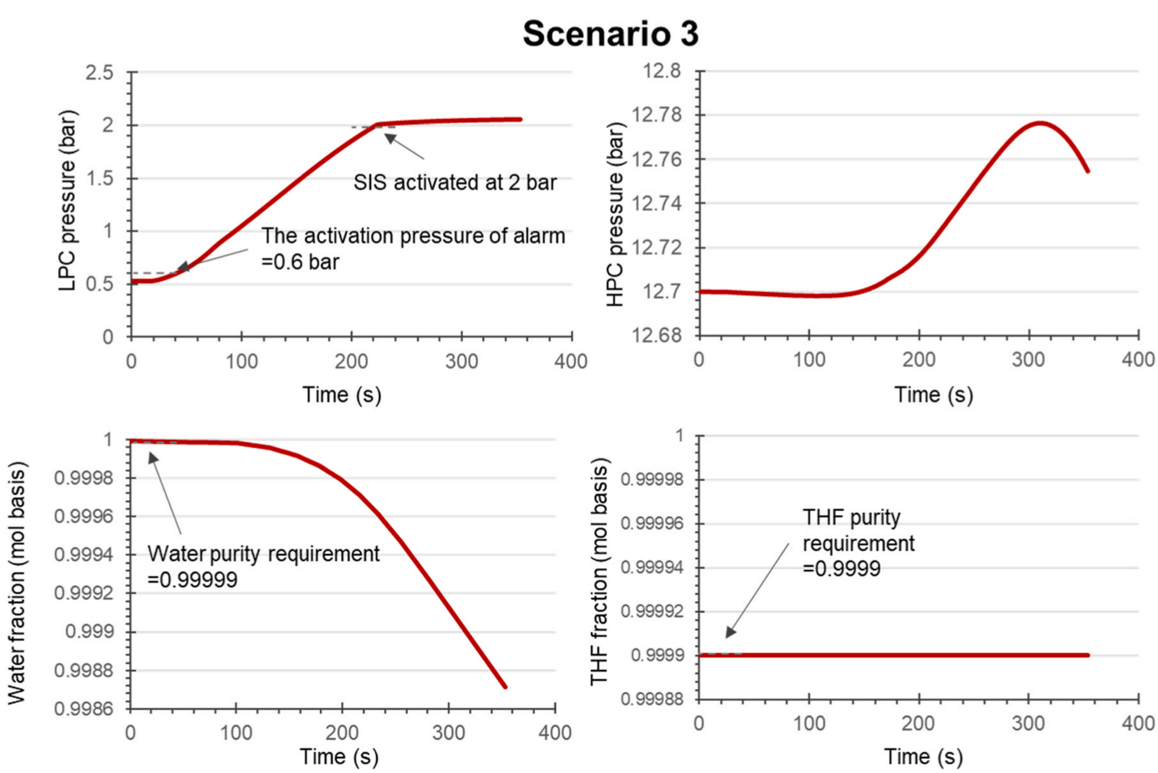

Fig. 10. Simulation results of Scenario 3.

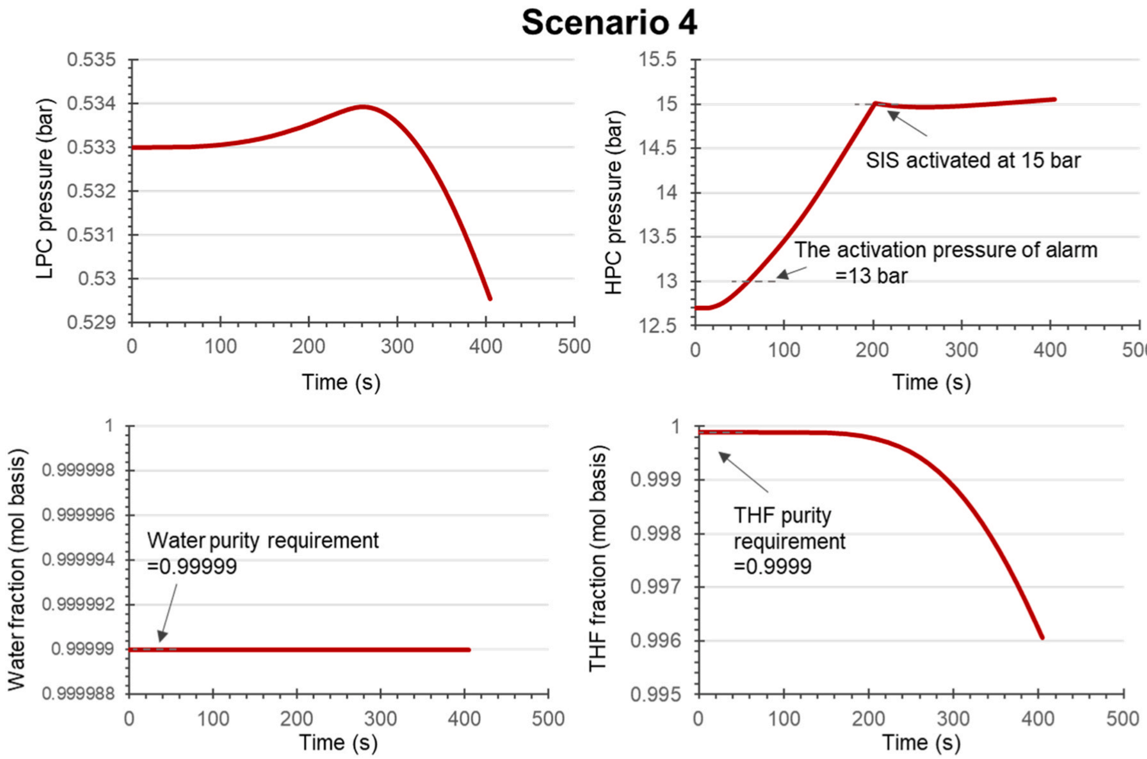

Fig. 11. Simulation results of Scenario 4.

Table 5
Pairwise comparison of the criterions (CPPs).

Score	LPC pressure	HPC pressure	Water fraction	THF fraction
HPC pressure	2	1	8	5
Water fraction	6	8	1	2

for pressure relief, which is 2.5 bar for water and 17 bar for THF. Table 2 summarizes the upper and lower limits for each CPP.

4.3. IPL analysis

The IPLs for mitigating the consequences of these disruptive scenarios must be identified before dynamic simulation and resilience quantification. The PSD process is equipped with IPLs such as the BPCS, hand valves for emergency response, the SIS, and PSVs. The BPCS is responsible for mitigating overpressure and column flooding, maintaining the CPPs within their corresponding normal operating ranges. Furthermore, the emergency valves, the SIS, and PSVs are set to mitigate overpressure. The complete flowsheet of the PSD process with its associated IPLs is shown in Fig. 6.

In case of overpressure corresponds to the loss of coolant or increased heat input, if the LPC or HPC reaches the high-pressure alarm setpoint of 0.6 or 13 bar, respectively, an alarm will be activated to notice the operators. The operator should be instructed to either lower the setpoint pressure or open the hand valve located in the coolant supply line to bypass the control valve (potentially faulty). If prompt human intervention is not taken, excessive heat accumulated in the column will cause the column pressure to continue to rise. Once the pressure reaches the activation setpoint of the SIS, the SIS will shut down the system by cutting off the feed and/or steam to the reboiler. There remains different options for configuring SIS regarding the combination of cutting off the feed and the steam. If SIS fails to respond, the PSV will be activated for pressure relief. Table 3 shows the activation pressure of each IPL, which is refer to our previous study.

In the case of column flooding caused by feed variations in either flow rate or composition, the BPCS—including feed flow rate control, reflux ratio control, and level controllers—mitigates column flooding. The SIS and PSVs are not involved in addressing flooding since the consequence is not severe and does not cause overpressure.

Considering the detailed configuration of IPLs, the aforementioned disruptions are further divided into several scenarios that provide more details on IPL activation for dynamic simulation. It should be noted that only the most severe disruption (D1) was selected for demonstration and case study. System resilience quantification is performed for each scenario. Table 4 summarizes the investigated scenarios.

4.4. Dynamic simulation and results

Dynamic simulations are conducted to obtain the time-varying results of system parameters. This study applied the simulation methodology developed in our previous research, which considered explicit heat transfer dynamics rather than simplified dynamics. The commercial software Aspen Plus V12 is used for steady-state simulation, and the results of the mass balance are used for sizing equipment, such as columns and drums. The steady-state system model is then updated to a pressure-driven dynamic system model using Aspen Dynamics V12. The established simulation model is shown in Fig. 7. Control loops and other IPLs, such as the SIS and PSVs, are added to the dynamic model. Readers can refer to Cui et al. (2023) for more simulation details. For each disruptive scenario, the simulation is run for the first 9 seconds at normal operating conditions, and then the disruption is introduced. The recording time interval of dynamic results of CPPs is 0.6 seconds.

Scenario 1. : Fig. 8 displays the simulation results of CPP changes over time for Scenario 1. Notably, the LPC pressure increases significantly following the loss of the cooling medium. The pressure escalation halts when the operator manually opens the cooling water valve after receiving the alarm at intervals of 30, 60, or 90 seconds. The LPC pressure reaches peaks of 0.82, 1.04, and 1.29 bar corresponding to these response times. Meanwhile, the HPC pressure shows only minor

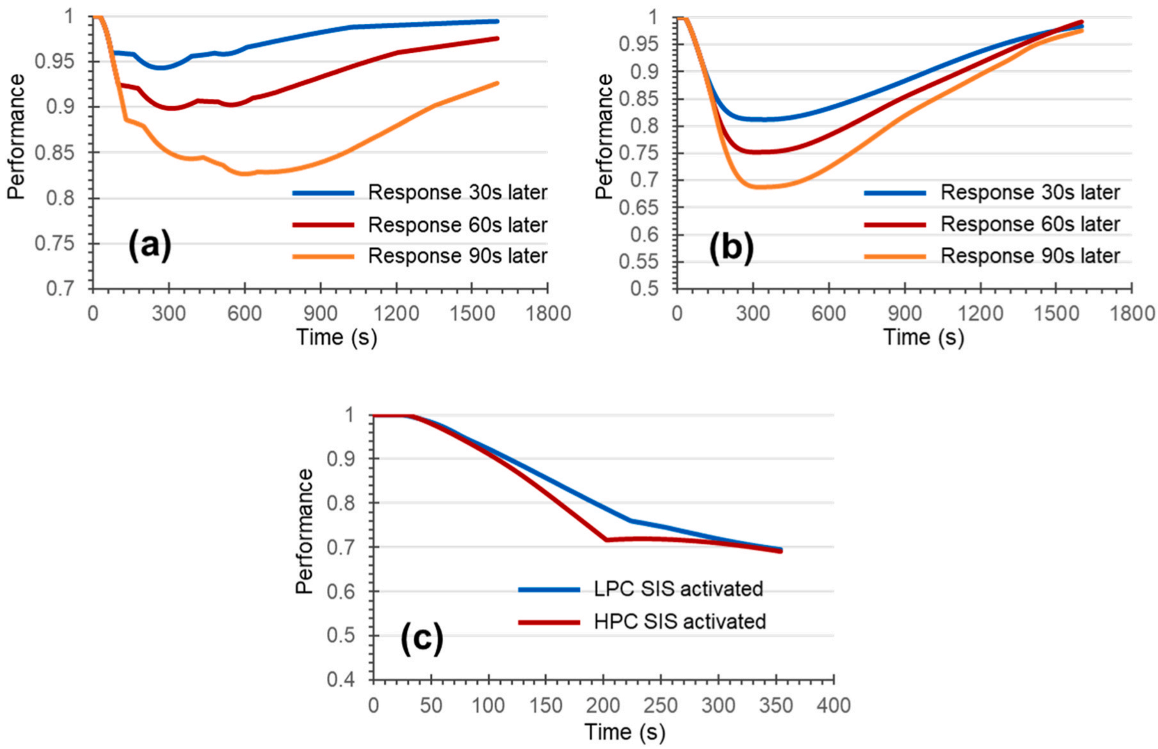

Fig. 12. System performance curve for each scenario: (a) for Scenario 1, (b) for Scenario 2, and (c) for Scenario 3 and Scenario 4.

fluctuations and stays below its alarm activation pressure. Effective operator actions help maintain control over the pressures, preventing the activation of the SIS and avoiding a process shutdown.

The water and THF fractions are crucial for monitoring process separation performance and assessing potential flooding effects. After the cooling medium is lost, the water fraction falls below the required purity level of 99.999 mol%. In the severe scenario where the operator's response is delayed to 90 seconds, the water fraction further decreases to 99.8 mol%. Conversely, the THF fraction increases, suggesting that the main product's quality remains unaffected.

Scenario 2. : Fig. 9 presents the simulation results of CPP changes over time for Scenario 2. In this scenario, the HPC pressure rises significantly after the loss of boiler water, and the increase ceases once the operator responds appropriately. The HPC pressure peaks at 14.26, 14.74, and 15.26 bar, respectively. The LPC pressure experiences minor fluctuations that do not significantly impact its performance. As a result, the water fraction remains nearly constant throughout the period. However, the THF fraction initially drops below the required purity level but recovers after the operator intervenes.

Scenario 3. : Fig. 10 presents the simulation results depicting changes in CPPs over time for Scenario 3. The LPC pressure increases almost linearly until the SIS activates, cutting the feeds and steam when the LPC pressure reaches 2 bar. Following the activation of the SIS, the LPC pressure is effectively managed and stabilizes at approximately 2 bar. The HPC pressure shows a slight increase as well, but it occurs with a delay relative to the LPC pressure before it begins to decrease. Throughout this period, the water fraction decreases, while the THF fraction remains steady.

Scenario 4. : Fig. 11 illustrates the simulation results of CPP changes over time for Scenario 4. Here, the HPC pressure rises nearly linearly until the SIS is activated to cut the steam when the HPC pressure reaches 15 bar. Following the activation of the SIS, the HPC pressure is effectively managed and stabilizes at approximately 15 bar. The LPC pressure experiences a slight increase but exhibits a delayed response compared to the HPC pressure before it begins to decrease. During this period, the THF fraction decreases while the water fraction remains constant.

4.5. Quantification of the system resilience

The dynamic simulation results of the considered disruptive scenarios are then utilized in quantifying the system resilience. For the four identified CPPs, the BWM is employed to determine the weights for each CPP, drawing on expert experience. During the expert scoring process for the CPPs, HPC pressure was identified as the most critical criterion (the best CPP), while the water fraction was identified as the least critical criterion (the worst CPP). The best and worst criteria are then compared pairwise with other criteria (CPPs). Table 5 presents the expert scoring results for these pairwise comparisons. The resulting weights for the LPC pressure, HPC pressure, water fraction, and THF fraction are 0.294, 0.529, 0.059, and 0.118, respectively.

After determining the weights for each CPP using the BWM based on expert input, the system performance curve is derived from the dynamic simulation results. Fig. 12 displays the system performance curve for each scenario. In Scenario 1, the system performance dips to 0.943, 0.899, and 0.826 at approximately 260, 307, and 590 seconds, respectively. Clearly, the later the operator responds, the faster the system performance drops, and the longer this reduced performance persists. Additionally, a delayed response prolongs the time required to restore system performance. In the most severe case, where the response is delayed by 90 seconds, the lowest performance remains above 0.8, and recovery to above 0.9 is achievable within 2500 seconds.

In Scenario 2, the system performance hits its lowest at 0.812, 0.752, and 0.688 at approximately 340, 305, and 322 seconds, respectively. Interestingly, despite different response times, the performance recovers to a similar level within the same period, highlighting the effectiveness of operator response as an IPL in restoring system performance from potential column overpressure. In Scenario 3, when the LPC SIS is activated at an LPC pressure of 2 bar, the performance drop is maintained at 0.760 but still gradually declines due to a decrease in the water fraction. Similarly, when the HPC SIS is activated at an HPC pressure of

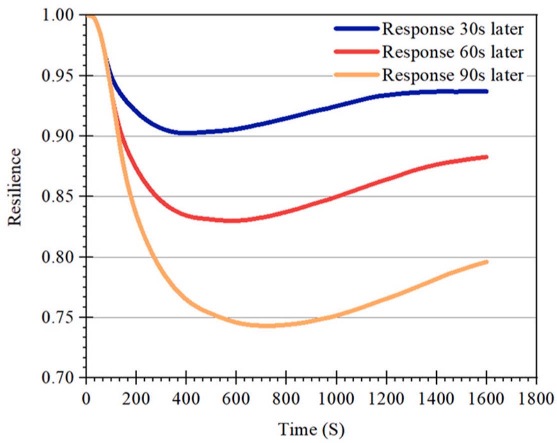

(*a*) The system resilience for Scenario 1

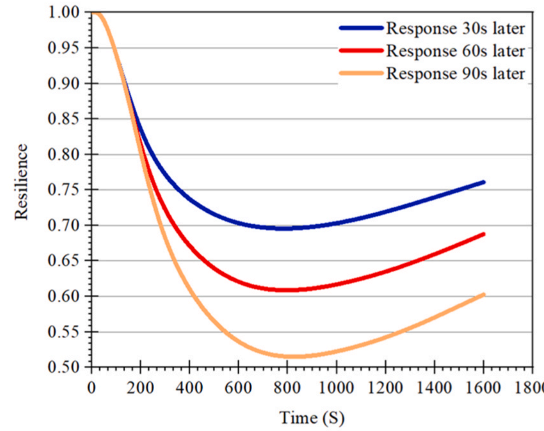

(*b*) The system resilience for Scenario 2

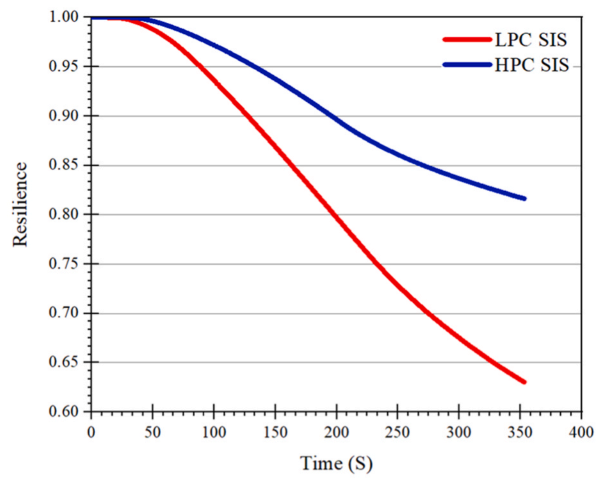

(*c*) The system resilience for Scenario 3 and Scenario 4

Fig. 13. System performance curve for each scenario.

Table 6
Comparison among different resilience assessment methods.

Method	Static assessment	Dynamic assessment	Single indicator	Multi indicator	Data uncertainty handling
Conceptual framework	√	×	×	×	×
semi-quantitative indices method	√	×	×	√	√
Deterministic method	×	√	√	×	×
Probabilistic method	×	√	√	×	√
The proposed method	×	√	×	√	√

15 bar, the performance is stabilized at 0.721 but continues to decline due to a decrease in the THF fraction. The control of system performance decline in both cases indicates that the system reaches the adaptation stage.

Finally, the resilience curve is obtained and Fig. 13 shows the system resilience curve for each scenario. From Fig. 13(a) and Fig. 13(b), it can be seen that, timely and effective alarm and response after alarm can effectively improve the system resilience. In other words, this is helpful for enhancing the ability of the system to cope with such non-desired events, and ensuring that the system can still have high performance under the influence of such disruptive events. Fig. 12(c) and Fig. 13(c) indicates that the presence of SIS can deal with the sharp rise in pressure in LPC and HPC. Obviously, SIS start-up thresholds can be optimized to cope with potential overpressure incidents. Thus, targeted measures should be taken to improve the resilience of the system to avoid accidents caused by such disruptions and scenarios. This part will be carried out in the future work.

4.6. Discussion

The resilience assessment methods for chemical process systems can be divided into two categories: qualitative and quantitative methods. Qualitative methods include conceptual frameworks and semi-quantitative indices. Conceptual frameworks help to understand system resilience and form the basis for quantitative evaluation, while semi-quantitative indices rely on expert evaluations of different aspects of system resilience. Quantitative methods typically measure system functionality or performance to quantify resilience, and include deterministic and probabilistic methods. In deterministic methods, uncertainty is not considered in the measurement (such as disturbance probabilities); whereas, probabilistic methods take into account the randomness associated with system behavior.

However, the above methods share a common issue, which is the uncertainty in data acquisition. To reduce the data and parameter uncertainty, the multiparametric resilience assessment of CPPs incorporating process dynamics and independent protection layers is proposed in the present work. The proposed method is able to dynamically assess the resilience of CPPs by considering the multi-dimensionality and time-varying characteristics of system parameters, while reducing data uncertainty. Table 6 presents the comparison among different resilience assessment methods.

In addition, the sensitivity analysis of the proposed method is also conducted. It can be seen from Fig. 12(a) and Fig. 12(b) that different response times affect the performance of the system. When the response time increases, the performance of the system decreases, but the overall curve shape and trend do not change. Similarly, Fig. 13(a) and Fig. 13(b) show that different response times affect the system resilience. When the response time increases, the system resilience decreases, but the overall curve shape and trend do not change.

5. Conclusions

Traditional resilience assessment methods often use reliability as the system performance indicators, but addressing the uncertainty and unavailability of reliability data remains a challenge in safety analysis. To tackle this, we propose a dynamic simulation-based, multiparametric resilience assessment method for CPSs. This method incorporates the influence of IPLs on system performance and resilience. It utilizes real-time process parameter as performance indicators, reflecting the impact of disruptions while reducing data uncertainty, thus quantifying system resilience and aiding decision-making for disruption management.

The resilience assessment approach was applied to a two-column PSD process. The results show the effectiveness of system protection across different disruption scenarios and intensities. It provides valuable insights for design and optimization of IPLs. This study also shows that improving system resilience against relatively frequent undesired disruption can prevent incidents from escalating into production accidents.

However, it is important to acknowledge the limitations of this study in terms of the model's robustness and the idealized nature of the selected case study. While the pressure-swing distillation process offers a clear example of the proposed method, challenges such as model convergence issues and the exclusion of real-world complexities—such as equipment degradation, operational variability, and non-ideal behavior—may impact the accuracy and generalizability of the resilience assessment. These factors could influence the propagation of disruptions and the subsequent system performance. Therefore, further research is needed to apply and refine this method across a broader range of CPSs, including those with more intricate operational dynamics and uncertainties. Incorporating these additional complexities will enhance the reliability of the resilience assessments and expand their applicability to real-world industrial processes.

CRediT authorship contribution statement

Yang Ming: Visualization, Validation, Supervision. **Qi Meng:** Software, Resources, Methodology. **Sun Hao:** Writing – original draft, Methodology, Investigation, Funding acquisition, Formal analysis, Data curation, Conceptualization. **Wang Heping:** Visualization, Validation, Investigation. **Wang Fuyu:** Software, Resources, Investigation, Formal analysis.

Declaration of Competing Interest

The co author, Ming Yang is an editor for the journal Process Safety and Environmental Protection, but has had no access to, or involvement in, the peer review process for this paper or its handling by the journal at any point.;

Acknowledgments

The authors gratefully acknowledge the financial support provided by the Anhui University of Technology Young Teachers Research Fund Project (QZ202315) and Anhui University of Technology Introduction of Talent Research Start-up Fund (QD202368) and Key Project of University Research Plan of Anhui Province (2024AH050162).

References

Amer, L., Erkoc, M., Celik, N., et al., 2023. Operationalizing resilience: a deductive fault-driven resilience index for enabling adaptation. Process Saf. Environ. Prot. 177, 1085–1102.
Aven, T., Zio, E., 2021. Globalization and global risk: How risk analysis needs to be enhanced to be effective in confronting current threats. Reliab. Eng. Syst. Saf. 205, 107270.
Bellè, A., Abdin, A.F., Fang, Y.P., et al., 2023. A data-driven distributionally robust approach for the optimal coupling of interdependent critical infrastructures under random failures. Eur. J. Oper. Res. 309, 872–889.
Cai, B.P., Zhang, Y.P., Wang, H.F., et al., 2021. Resilience evaluation methodology of engineering systems with dynamic-Bayesian-network-based degradation and maintenance. Reliab. Eng. Syst. Saf. 209, 107464.
Chen, C., Li, J., Zhao, Y.X., et al., 2023. Resilience assessment and management: a review on contributions on process safety and environmental protection. Process Saf. Environ. Prot. 170, 1039–1051.
Cincotta, S., Khakzad, N., Cozzani, V., et al., 2019. Resilience-based optimal firefighting to prevent domino effects in process plants. J. Loss Prev. Process Ind. 58, 82–89.
Cui, C., Long, N.V.D., Sun, J., et al., 2020. Electrical-driven self-heat recuperative pressure-swing azeotropic distillation to minimize process cost and CO2 emission: process electrification and simultaneous optimization. Energy 195, 116998.
Cui, C.T., Qi, M., Shu, C.M., et al., 2023. Rigorous dynamic simulation methodology for scenario-based safety analysis of pressure-swing distillation considering independent protections. Process Saf. Environ. Prot. 172, 282–304.
Dowell III, A.M., 2019. Understanding IPL boundaries. Process Saf. Prog. 38 (2), e12019.
Hoseyni, S.M., Cordiner, J., 2024. A novel framework for quantitative resilience assessment in complex engineering systems during early and late design stages. Process Saf. Environ. Prot. 94, 172–179.
Hu, J.Q., Dong, S.H., Zhang, L.B., et al., 2021. Cyber-physical-social hazard analysis for LNG port terminal system based on interdependent network theory. Saf. Sci. 137, 105180.
Jain, P., Rogers, W.J., Pasman, H., et al., 2018. A resilience-based integrated process systems hazard analysis (RIPSHA) approach: Part I plant system layer. Process Saf. Environ. Prot. 148, 92–105.
Janošovský, J., Danko, M., Labovský, J., Jelemenský, Ľ., 2017. The role of a commercial process simulator in computer aided HAZOP approach. Process Saf. Environ. Prot. 107, 12–21.
Kamil, M.Z., Khan, F., Halim, S.Z., et al., 2023. A methodical approach for knowledge-based fire and explosion accident likelihood analysis. Process Saf. Environ. Prot. 107, 12–21.
Khan, F., Amyotte, P., 2007. Modeling of BP Texas city refinery incident. J. Loss Prev. Process Ind. 20, 387–395.
Khan, F., Yarveisy, R., Abbassi, R., 2021. Risk-based pipeline integrity management: a road map for the resilient pipelines. J. Pipeline Sci. Eng. 1, 74–87.
Kister, H.Z., 1997. Are column malfunctions becoming extinct—or will they persist in the 21st century? Chem. Eng. Res. Des. 75 (6), 563–589.
Ko, C., Lee, H., Kim, K., Lee, W.B., 2020. Quantitative risk assessment integrated with dynamic process simulation for reactor section in heavy oil desulfurization process. J. Loss Prev. Process Ind. 66, 104158.
Kummer, A., Varga, T., 2019. Process simulator assisted framework to support process safety analysis. J. Loss Prev. Process Ind. 58, 22–29.
Lee, J., Cameron, I., Hassall, M., 2024. Dynamic simulation for process hazard analysis: affordances and limitations in the application to complex process systems. J. Loss Prev. Process Ind. 87, 105232.
Leveson, N.G., Stephanopoulos, G., 2014. A system-theoretic, control-inspired view and approach to process safety. AIChE J. 60, 2–14.
Li, X.H., Liu, Y.Z., Abbassi, R., et al., 2022. A Copula-Bayesian approach for risk assessment of decommissioning operation of aging subsea pipelines. Process Saf. Environ. Prot. 167, 412–422.
Li, X.H., Liu, Y.B., Han, Z.Y., Chen, G.M., 2024. A risk-based maintenance decision model for subsea pipeline considering pitting corrosion growth. Process Saf. Environ. Prot. 184, 1306–1317.
Li, X.H., Ma, J., Pasman, H., et al., 2023. Dynamic risk investigation of urban natural gas pipeline accidents using Stochastic Petri net approach. Process Saf. Environ. Prot. 178, 933–946.

Liu, X., Wang, C., Yin, Z., An, X., Meng, H., 2024. Risk-informed multi-objective decision-making of emergency schemes optimization. Reliab. Eng. Syst. Saf. 245, 109979.
Luyben, W.L., 2012. Rigorous dynamic models for distillation safety analysis. Comput. Chem. Eng. 40, 110–116.
Meng, H., An, X., Li, D., et al., 2024. A STAMP-Game model for accident analysis in the oil and gas industry. Pet. Sci. 21, 2154–2167.
Misuri, A., Cozzani, V., 2021. A paradigm shift in the assessment of Natech scenarios in chemical and process facilities. Process Saf. Environ. Prot. 152, 338–351.
Ouyang, M., Liu, C., Xu, M., 2019. Value of resilience-based solutions on critical infrastructure protection: comparing with robustness-based solutions. Reliab. Eng. Syst. Saf. 190, 106506.
Pasman, H., Sripaul, E., Khan, F., et al., 2023. Energy transition technology comes with new process safety challenges and risks. Process Saf. Environ. Prot. 177, 765–794.
Pawar, B., Huffman, M., Khan, F., et al., 2022. Resilience assessment for fast response process systems. Process Saf. Environ. Prot. 163, 82–93.
Qian, Y.T., Vaddiraju, S., Khan, F., 2024. Inherent process risk index (IPRI) – a tool for analyzing inherently safer design using aspen plus simulation. Process Saf. Environ. Prot. 183, 399–416.
Reniers, G., Khakzad, N., Cozzani, V., et al., 2018. The impact of nature on chemical industrial facilities: dealing with challenges for creating resilient chemical industrial parks. J. Loss Prev. Process Ind. 56, 378–385.
Rezaei, J., 2015. Best-worst multi-criteria decision-making method. Omega 53, 49–57.
Sharma, N., Tabandeh, A., Gardoni, P., 2018. Resilience analysis: a mathematical formulation to model resilience of engineering systems. Sustain. Resilient Infrastruct. 3, 49–67.
Sun, H., Yang, M., Wang, H., 2022. Resilience-based approach to maintenance asset and operational cost planning. Process Saf. Environ. Prot. 162, 987–997.
Sun, H., Yang, M., Wang, H., 2024. An integrated approach to quantitation resilience assessment in process systems. Reliab. Eng. Syst. Saf. 243, 109878.
Szatmári, K., Németh, S., Kummer, A., 2024. Integration of resilience engineering and reinforcement learning in chemical process safety. Process Saf. Environ. Prot. 181, 343–353.
Tang, Y.C., Bi, W., Varga, L., et al., 2022. An integrated framework for managing fire resilience of metro station system: identification, assessment, and optimization. Int. J. Disaster Risk Reduct. 77, 103037.
Tong, Q., Gernay, T. Resilience assessment of process industry facilities using dynamic Bayesian networks. Process Safety and Environmental Protection, 169, 547-563.
Wang, Y.C., Henriksen, T., Deo, M., et al., 2021. Factors contributing to US chemical plant process safety incidents from 2010 to 2020. J. Loss Prev. Process Ind. 71, 104512.
Wen, H., Khan, F., 2024. A risk-based model for human-artificial intelligence conflict resolution in process systems. Digit. Chem. Eng. 13, 100194.
Wu, Q., Liu, X.W., Zhou, L.G., et al., 2024. An analytical framework for the best-worst method. Omega 123, 102974.
Xu, M., Li, G.Y., Chen, A., 2024. Resilience-driven post-disaster restoration of interdependent infrastructure systems under different decision-making environments. Reliab. Eng. Syst. Saf. 241, 109599.
Yan, R.D., Dunnett, S., Andrews, J., 2023. A Petri net model-based resilience analysis of nuclear power plants under the threat of natural hazards. Reliab. Eng. Syst. Saf. 230, 108979.
Yang, M., Sun, H., Geng, S.Y., 2023. On the quantitative resilience assessment of complex engineered systems. Process Saf. Environ. Prot. 174, 941–950.
Yazdi, M., Khan, F., Abbassi, R., Quddus, N., 2022. Resilience assessment of a subsea pipeline using dynamic Bayesian network. J. Pipeline Sci. Eng. 2, 100053.
Yazdi, M., Zarei, E., Pribalouti, R.G., Li, H., 2024. A comprehensive resilience assessment framework for hydrogen energy infrastructure development. Int. J. Hydrog. Energy 51, 928–947.
Zarei, E., Khan, F., Abbassi, R., 2023. An advanced approach to the system safety in sociotechnical systems. Saf. Sci. 158, 105961.
Zarei, E., Yazdi, M., Moradi, R., Bahootoroody, A., 2024. Expert judgment and uncertainty in sociotechnical systems analysis. Safety Causation Analysis in Sociotechnical Systems: Advanced Models and Techniques. Springer Nature Switzerland, Cham, pp. 487–530.
Zeng, T., Chen, G.H., Reniers, G., et al., 2022. Developing a barrier management framework for dealing with Natech domino effects and increasing chemical cluster resilience. Process Saf. Environ. Prot. 168, 778–791.
Zhang, Y.P., Cai, B.P., Ahmed, S., Wang, C., Li, Q.P., Gao, L., 2025. A resilience-driven emergency maintenance operation scheme optimization method based on risk. Reliab. Eng. Syst. Saf. 254, 110630.
Zhu, C.L., Qi, M., Jiang, J.C., 2020. Quantifying human error probability in independent protection layers for a batch reactor system using dynamic simulations. Process Saf. Environ. Prot. 133, 243–258.
Zio, E., 2018. The future of risk assessment. Reliab. Eng. Syst. Saf. 177, 176–190.
Zio, E., 2022. Prognostics and Health Management (PHM): where are we and where do we (need to) go in theory and practice. Reliab. Eng. Syst. Saf. 218, 108119.